frontiers
IN NEUROSCIENCE

Persistently active, pacemaker-like neurons in neocortex

Morgane Le Bon-Jego[a] **and Rafael Yuste***

HHMI, Department of Biological Sciences, Columbia University, New York, NY, USA

Review Editors: Yosef Yarom, Dept. of Neurobiology and Interdisciplinary Center for Neural Computation, Hebrew University, Israel
Henry Markram, Brain Mind Institute, Ecole Polytechnique Fédéral de Lausanne, Switzerland

The neocortex is spontaneously active, however, the origin of this self-generated, patterned activity remains unknown. To detect potential "pacemaker cells," we use calcium imaging to directly identify neurons that discharge action potentials in the absence of synaptic transmissionin slices from juvenile mouse visual cortex. We characterize 60 of these neurons electrophysiologically and morphologically, finding that they belong to two classes of cells: one class composed of pyramidal neurons with a thin apical dendritic tree and a second class composed of ascending axon interneurons (Martinotti cells) located in layer 5. In both types of neurons, persistent sodium currents are necessary for the generation of the spontaneous activity. Our data demonstrate that subtypes of neocortical neurons have intrinsic mechanisms to generate persistent activity. Like in central pattern generators (CPGs), these neurons may act as "pacemakers" to initiate or pattern spontaneous activity in the neocortex.

Keywords: CPG, Martinotti, persistent sodium, FAP

INTRODUCTION

Neocortical circuits are spontaneously active *in vivo* (Llinás, 2001; Steriade et al., 1993; Sanchez-Vives and McCormick, 2000; Kenet et al., 2003) and *in vitro* (Mao et al., 2001; Cossart et al., 2003; Sanchez-Vives and McCormick, 2000; Ikegaya et al., 2004). The fact that this activity persists in isolated neocortical slices, in the absence of any input, or electrical or pharmacological stimulation, means that it must be generated by the cortical mircrocircuit. This persistent activity is also not a stochastic process but instead shows a precise spatial and temporal structure (Grinvald et al., 2003; Cossart et al., 2003; Ikegaya et al., 2004).

In spite of its prevalence, the function of the spontaneous activity is still unknown. These reverberations probably reflect in some way the connectivity of the underlying microcircuits. Moreover, as Lorente de Nó proposed, the highly recurrent nature of cortical circuits suggests that the generation of reverberating activity could be the main function of the neocortex (Lorente de Nó, 1938). In addition, it has been proposed that spontaneous rhythmic activity could reflect a basic information processing of cortical circuits or perhaps mental states (Llinás, 2001). Finally, persistent activity has also been linked to working memory (Goldman-Rakic, 1995; Wang, 2001) and neuronal integration (Aksay et al., 2001).

The mechanisms that generate this endogeneous, persistent activity in the cortex are controversial. On the one hand, some neurons in archicortex have intrinsic mechanisms that can generate persistent activity under cholinergic stimulation (Egorov et al., 2002). Thus, like central pattern generators (CPGs) in other systems (Kiehn and Butt, 2003; Marder, 2000), neocortical spontaneous activity could be driven by pacemaker cells (Llinás, 1987; Llinás, 2001). On the other hand, it has been proposed that in the neocortex, persistent cortical activity could result from circuit mechanisms, arising from a careful balance of excitation and inhibition (Brunel and Wang, 2003; Shu et al., 2003).

Here, we introduce a novel assay to detect potential pacemaker cells in circuits. Specifically, we have taken advantage of the single-cell resolution of calcium imaging to directly search for persistently active neurons in cortical circuits *in vitro*, by monitoring spontaneous spiking activity in a large population of neocortical neurons in order to detect those neurons that are spontaneously active, after pharmacologically blocking all excitatory and inhibitory synapses. We indeed find neurons that are capable of exhibiting spontaneous activity in the absence of synaptic input. Physiological and morphological characterization revealed that these cells belong to two main classes of neurons: a thin pyramidal type and a class of interneurons with ascending axons, traditionally classified as Martinotti cells. We investigate the intrinsic mechanisms that enable them to fire in the absence of synaptic inputs and find that persistent sodium currents are necessary for their spontaneous activity. Our results demonstrate that neocortical circuits are endowed with ''pacemaker''-like neurons and are thus consistent with the hypothesis that the cortex may represent the encephalization of CPGs (Llinás, 2001).

MATERIALS AND METHODS

Slice preparation

Cortical slices from P14-P17 C57B1/6 mouse primary visual cortex were prepared as described previously (Peterlin et al., 2000). Briefly, animals were anesthetized with an intraperitoneal injection of a mixture of 100 mg/kg ketamine and 5 mg/kg xylaxine and decapitated. The brains were rapidly removed and transferred into an ice-cold sucrose solution bubbled with 95% O_2 and 5% CO_2 with the following composition (in mM): 222 sucrose, 2.6 KCl, 27 $NaHCO_3$, 1.5 NaH_2PO_4, 0.5 $CaCl_2$, 7 $MgSO_4$, and 0.1 ascorbic acid. Slices (350 μm-thick) were cut with a Leica vibratome (VT1000S) and transferred to a submerged slice chamber in normal ACSF that consisted of: 123 mM NaCl, 3.5 mM KCl, 26 mM $NaHCO_3$, 1 mM NaH_2PO_4, 1.2 mM $CaCl_2$, 1 mM $MgSO_4$, and 10 mM dextrose for 45 min.

* Correspondence: Rafael Yuste, Columbia University, Biological Sciences, 1002 Fairchild Center, M.C. 2435, New York, N.Y. 10027.

[a] Current address: Universités Bordeaux 2, 1, Centre National de la Recherche Scientifique, Unité Mixte de Recherche 5227, Bordeaux, F-33076, France.

Received: 15 August 2007; paper pending published: 01 September 2007; accepted: 01 September 2007; published online: 15 October 2007.

Full citation: Frontiers in Neuroscience. (2007) vol. 1, iss. 1,123-129.

Bulk loading and imaging

Slices were then bulk loaded with the calcium indicator dye Oregon-Green 488 Bapta-1 (Molecular Probes, special packages) as previously described (Ikegaya et al., 2005). The 50 μg of the dye was dissolved in 8 μL of 0.5% Cremophor EL/DMSO and 2 μL of 10% pluronic acid or in 15 μL of DMSO and 2 μL of 10% pluronic acid, and then added to 3 mL of ACSF. Slices were transferred to this solution and kept in the dark at 37 °C for 45 minutes with constant oxygenation. After the loading, slices were placed in the submerged slice chamber and slices were imaged after 45 minutes. For imaging slices, slices were transferred to a submerged recording chamber. We used a spinning disk confocal microscope (Perkin-Elmer Ultraview; Olympus BX50WI, Hamamatsu ORCA-ER CCD camera). 20X/ and 40X/0.8NA water immersion objectives were used to scan areas of 448 × 341 μm^2 and 224 × 170 μm^2, respectively. Frame rate was typically 5 frames per second and the duration of the movie was usually between 1 and 5 minutes. For signal extraction, all frames of a movie were collapsed into a single image by averaging fluorescence intensity with the max-intensity mode of Z-projection stacking in the free software Image J (National Institutes of Health) and Matlab (MathWorks). Cell contours were automatically detected using a custom algorithm. The averaged fluorescence of each pixel inside each contour was read for each frame of the movie. To detect individual optical events, the fluorescence change over time was defined as $\Delta F/F = (F - F_{basal})/F_{basal}$, where F is the fluorescence at any point, and F_{basal} the baseline fluorescence averaged across the whole movie for each cell. The bleaching was removed by detrending the signal with a first order polynomial function.

Electrophysiology

For somatic whole-cell recordings, neurons were selected in V1 based on their calcium dynamics. Microelectrodes (6–10 MΩ) were filled with the following intracellular recording solution (in mM): 5 NaCl, 10 KCl, 10 K-Hepes, 130 K-$MeSO_4$, 2.5 Mg-ATP, 0.3 Na-GTP, and 0.5% biocytin (pH = 7.2, 296 mOsm). Recordings were done at room temperature or at 37 °C. For homogeneity, all data presented in the figures and quantified in the tables and the text were from experiments made at room temperature. Signals were amplified using an amplifier (ECP10; Heka Electronic), sampled at 5–10 Hz, filtered at 1–2 KHz and stored onto the hard disk of a PC for offline analysis using custom software (Igor or Matlab). All spontaneously active neurons were healthy, as evident by their resting membrane potential, action potential kinetics and repolarizations, all similar to those reported by other groups *in vitro* and *in vivo* (**Table 1**). Thus, we do not believe that the spontaneous active neurons were active due to cellular damage. Characterization of neurons was based on their responses to a series of somatic current injections protocol in current-clamp mode. Intracellular application of prolonged (400 ms) depolarizing and hyperpolarizing current pulses were used. We analyzed the shape of action potential, the discharge response to step current pulses around threshold of increasing amplitude and sag or/and rebound spike produced by different hyperpolarization current pulse of increasing amplitude. Input resistance was measured by hyperpolarizing current pulses (amplitude −40 pA, duration 400 ms). Ratio of second, fourth, and last spike interval time to the first when spike frequency of the first one was 25–50 and 50–100 Hz gave the degree of spike frequency adaptation. The amplitude of spike was measured from the threshold to the peak of spike on spontaneous action potentials. Their duration was measured at half amplitude. The amplitude of the AHP was measures between the spike threshold and the most negative level reached during the repolarization phase. All data is expressed as mean ± SD, unless noted. Significance of differences ($p < 0.05$) was assessed using Student's *t*-test.

Synaptic blockers

We used 2-amino-5-phosphonovaleric acid (APV, 75–100 μM), 6-cyano-7-nitroquinoxaline-2,3-dione (CNQX, 40–50 μM), or 1,2,3,4-tetrahydro-6-nitro-2,3-dioxo-benzo[f]quinoxaline-7-sulfonamide disodium salt (NBQX, 10–20 μM) to block NMDA and non-NMDA glutamatergic receptors and either picrotoxin (75–100 μM) or gabazine (10–20 μM) to block $GABA_A$ receptors. No apparent differences were found between picrotoxin or gabazine results. We used these relatively high concentrations of synaptic blockers in order to ensure a complete blockade of fast GABAergic and glutamatergic synaptic neurotransmission. In all the movies, the complete disappearance of ensemble activity in the presence of synaptic blockers confirmed the efficiency of the blockers. Finally, inspection of intracellular recording revealed that spontaneous EPSPs and IPSPs were absent confirming that the synaptic blockers were effective at the concentrations used. We also used Riluzole (5 μM) to block the persistent sodium current.

Morphology

Neurons were filled with biocytin by diffusion from the intrapipette solution during recordings. At the end of each recording, slices were fixed overnight in 4% paraformaldehyde. Thereafter, slices were rinsed several times in 0.12 M phosphate buffer (PB) saline. Slices were then transferred in 30% sucrose in 15 mL of 0.12 M PB for at least 2 hours and as long as one week. Slices were then frozen in an embedding medium. After freezing, slices were rinsed in 0.12 M PB several times. Slices were then incubated in H_2O_2 1% in 0.12 M PB for 30 minutes under agitation and rinsed in 0.12 M PB once for 15 minutes. After two other washes in 0.02 M KPBS, the slices were incubated overnight under agitation in 1% avidin–biotin complex (ABC Kit Standard, Vector Laboratories) prepared in 0.3% Triton X-100. After three rinses in PB, bicoytin was revealed by the diaminobenzidine. After two final rinses in PB, slices were mounted onto slides. The neurons were reconstructed in three dimensions with Neurolucida (Micro Bright Field Inc., USA).

RESULTS

Detecting persistently active neurons in neocortical slices

We used coronal slices from primary visual cortex (V1) of juvenile (P14-20) mice, and bulk loaded them with the calcium indicator Oregon Green 488-Bapta-1 AM (**Figure 1A**; see Methods). We took advantage of the correspondence between action potential generation and somatic calcium transients (Yuste and Katz, 1991; Smetters et al., 1999) to detect the action potential activity of the entire imaged population of neurons. Using a spin-disk confocal microscope at 100 or 200 ms/frame, we imaged the spontaneous calcium activity of several hundreds to a thousand cells per imaged field and then applied automatic online algorithms to analyze the movies, detect all the cells and quickly identify those that were active. As described previously (Cossart et al., 2003, Ikegaya et al., 2004), we encountered spontaneous synchronizations of ensembles of neurons, often located in particular regions of the imaged territories (**Figure 1B**-red cells).

We then blocked both excitatory and inhibitory transmission in these slices, by combined bath application of glutamatergic and GABAergic antagonists (APV/CNQX/picrotoxin or APV/NBQX/Gabazine) and repeated the imaging protocols to detect neurons that were still spontaneously active in the absence of synaptic transmission (**Figure 1C**). Indeed, in all experiments and in all slices we found neurons that displayed robust spontaneous activity in spite of the synaptic blockers, although co-activations of ensembles of neurons were not encountered anymore. We then identified those spontaneously active neurons following blockade of synaptic transmission and characterized their somatic calcium dynamics (**Figure 1D**). The analysis of their spontaneous calcium transients revealed that these cells exhibited persistent activity, characterized by either relatively long and irregular calcium transients with rapid onset (**Figure 1D1**) or calcium transients occurring regularly (**Figure 1D2**; Supplemtal Data Movie 1). Up to six cells, that could be sparsely or closely located, could be imaged in the same field of view (450 × 340 μm^2).

We then selected those cells with more prominent spontaneous activity in the calcium imaging for further study, and used whole-cell current-

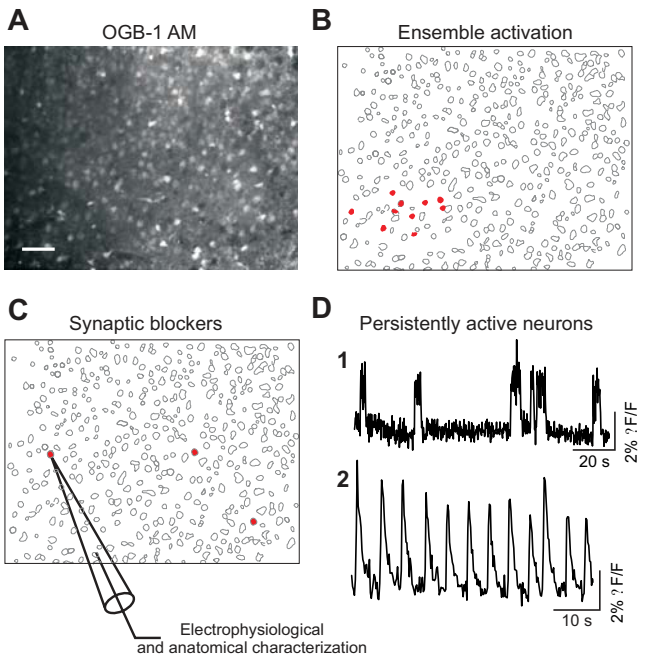

Figure 1. Optical detection of intrinsically active neurons. *(**A**) Confocal image of Oregon green BAPTA 1 (OGB-1 AM) loading of a brain slice of mouse primary visual cortex. Scale bar: 50 μm. (**B**) Map showing representative spontaneous coactivations of neurons observed in control condition characterized. Red cells are active neurons. (**C**) Map showing the position of three cells (in red) displaying persistent activity in the presence of synaptic blockers. Targeted whole-cell recordings of these persistently active neurons were performed for electrophysiological and morphological characterization. (**D**) Representative calcium transients of persistently active neurons observed after synaptic transmission blockade. (**D1** and **D2**) Time resolution, 200 ms per frame.*

clamp recordings to successfully characterize 60 of them morphologically and electrophysiologically. The electrophysiological recordings of the spontaneously active cells detecting by calcium imaging confirmed that all targeted cells were neurons and that they were capable of spontaneously firing action potentials in the absence of synaptic input. Moreover, the intracellular analysis of the intrinsically active neurons revealed them as healthy cells, as evidenced from their normal electrophysiological properties (Table 1), ruling out potential artifacts introduced by the slicing or calcium indicator loading procedures.

A subtype of pyramidal neurons is spontaneously active

Cells that were spontaneously active in the presence of synaptic blockers fell within two distinct categories of neurons, which differed in morphology, evoked firing patterns and patterns of spontaneous activity. The most commonly found type of persistently active cells were a subtype of pyramidal neurons located in layers 2/3 and 5 ($n = 25$; Figure 2). No significant differences were found between neurons located in these two different layers, so their analysis was pooled. These intrinsically active neurons displayed episodic sequences of action potential activity (Figure 2A). Basic electrophysiological properties (see Table 1) were evaluated for 20 cells, all of which presented very similar characteristics. Specifically, neurons had a normal resting potential (∼−62 mV) and responded to intracellular injection of depolarizing current pulses with sustained repetitive firing, and displayed a brief burst with relatively little accommodation with increasing current injection (Figure 2B1; see table; ''Burst-non adapting'' in the Petilla electrophysiological nomenclature, see http://www.columbia.edu/cu/biology/faculty/yuste/petilla/petilla-webpages/classification/classification.htm). In these cells, a sag (Ih current) was also evident in response to hyperpolarizing current injection and post-inhibitory rebound (Figure 2B2) was also observed at the offset of hyperpolarizing current injection and in most cases reached the spike threshold.

This class of neurons was morphologically analyzed post-hoc. The reconstruction of these cells revealed pyramidal morphologies (Figure 2C; Kawaguchi and Kubota, 1993; Tsiola et al., 2003). Somata were relatively small and had a pyramidal shape with a distinct apical dendrite, which was thin and with relatively few or no branches, before ending in layer 1. Bundles of basal dendrites were found in the layer of the soma. These pyramidal cells had axons that projected to the upper layers within the same cortical area (Figures 2C1 and 2C2, red) and, in some cases, also had distant projections that left the slice (Figure 2C2). In layer 5, these cells were similar to the ''subgroup 3'' type of mouse V1 pyramidal neuron, discriminated in our previous cluster analysis studies (''narrow pyramidal neurons''; Tsiola et al., 2003), and different from the large layer 5 pyramidal cells which we have previously characterized in mouse V1 (Kozloski et al., 2001; Tsiola et al., 2003).

Martinotti layer 5 interneurons are spontaneously active

Using the same experimental approach, a second type of neuron was found, located exclusively in layer 5, that also displayed spontaneous, but in this case, strikingly regular, activity (Figure 3). Calcium imaging movies revealed cells that generated pacemaker-like calcium transients, i.e., consistent and regular (Figure 1D2). Very few cells were found in each imaged field. Targeted patch-clamp recording of 35 of these cells revealed regular bursts of action potentials, corresponding with an underlying oscillation in

Table 1. Electrophysiological characteristics of the two categories of neurons displaying persistent activity in neocortex.

	Type 1 Pyramidal cells	Type 2 interneurons
Resting potential (mV)	−62.4 ± 2.23 ($n = 20$)	−66.78 ± 1.56 ($n = 10$)
Input resistance (MΩ)	522.1 ± 160.1 ($n = 18$)	474.4 ± 160.7 ($n = 9$)
Action potential amplitude (mV)	86.14 ± 9.22 ($n = 17$)	89.81 ± 13 ($n = 10$)
Duration at mid-height (ms)	1.57 ± 0.35 ($n = 17$)	0.82 ± 0.196 ($n = 10$)
AHP amplitude (mV)	19.07 ± 1.71 ($n = 17$)	11.83 ± 4 ($n = 10$)
Second spike interval/first spike interval (25–50 Hz)	1.33 ± 0.16 ($n = 17$)	1.05 ± 0.16 ($n = 8$)
Fourth spike interval/first spike interval (25–50 Hz)	1.70 ± 0.38 ($n = 17$)	1.17 ± 0.34 ($n = 8$)
Last spike interval/first spike interval (25–50 Hz)	2.07 ± 0.79 ($n = 17$)	1.77 ± 0.67 ($n = 8$)
Second spike interval/first spike interval (50–100 Hz)	1.57 ± 0.35 ($n = 17$)	1.03 ± 0.14 ($n = 8$)
Fourth spike interval/first spike interval (50–100 Hz)	1.93 ± 0.32 ($n = 17$)	1.19 ± 0.18 ($n = 8$)
Last spike interval/first spike interval (50–100 Hz)	2.39 ± 0.46 ($n = 17$)	2.06 ± 0.53 ($n = 8$)

Data are mean ± SD; n = number of cells.

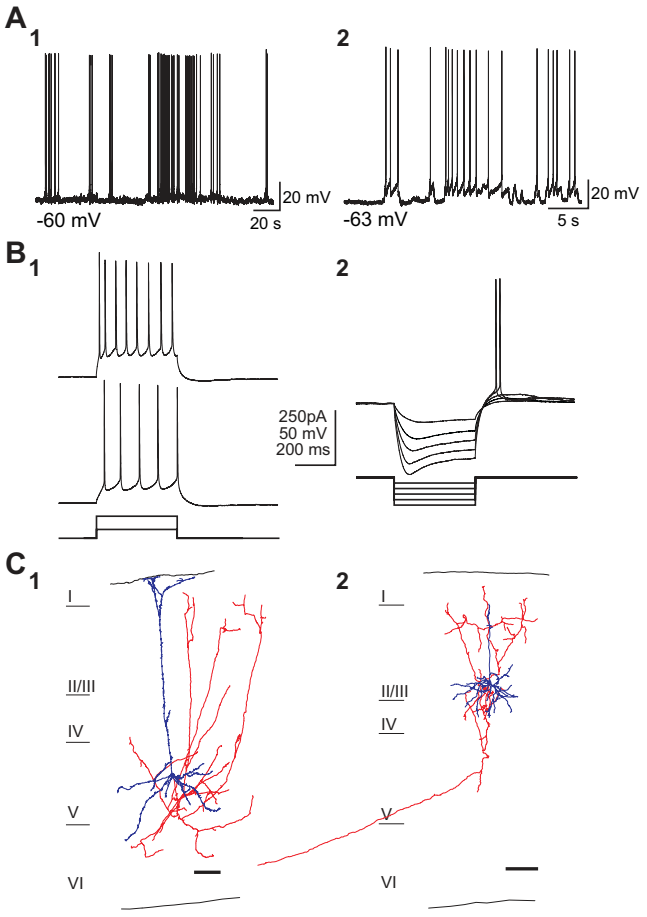

Figure 2. A subtype of pyramidal cells are intrinsically active. *(**a**) Current-clamp recordings of two spontaneously active cells of the first subtype (**A1**, **A2**) in the presence of APV, CNQX, and Picrotoxin. (**b**) Responses to somatic depolarizing (B1) and hyperpolarizing (**B2**) current pulses. Note the spiking behavior with small adaptation and typical voltage sag during hyperpolarization and rebound spike immediately following the current pulse. (**C**) Anatomical reconstruction of two biocytin-filled spontaneously active cells in layer 5 and layer 2/3 (**C1** and **C2**). Cell body and dendrites are colored blue, and axon red. Note the typical pyramidal somata and apical dentritic trees as well as the typical pyramidal axonal projections. Scale bar, 100 μm. Cell bodies and dendrites in blue and axons in red.*

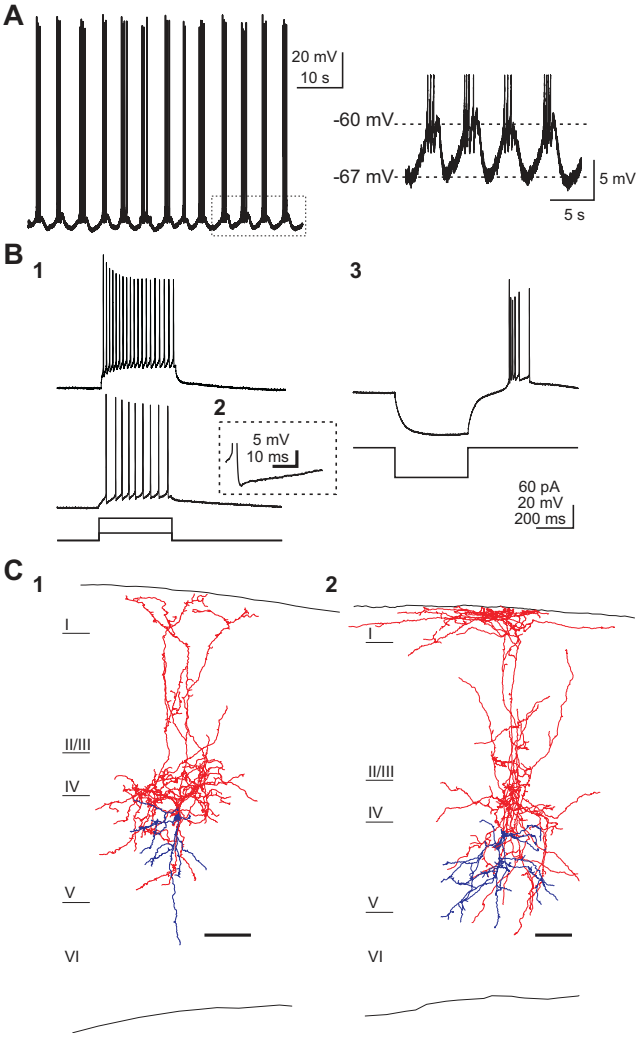

Figure 3. A subtype of layer 5 interneurons are intrinsically active. *(**A**) Current clamp recording of a spontaneously active cell displaying regular burst of action potentials modulated by a underlying oscillation in membrane potential (right) in the presence of synaptic blockers. (**B**) Small depolarizing current steps (20 pA, 400 ms) are required for firing this low-threshold spiking cells (**B1**). Note the complex AHP shape (**B2**) and the rebound burst (**B3**) after a hyperpolarizing current injection (−50 pA, 400 ms) typical to LTS interneurons. (**C**) Anatomical characterization of the pacemaker-like cells reveals typical ascending axon/Martinotti cell morphology localized in layer 5. Scale bar, 100 μm. Cell bodies and dendrites in blue and axons in red.*

membrane potential (Figure 3A). These oscillations were present in the absence of any current injection or pharmacological manipulation. The frequency and amplitude of these membrane potential oscillations underlying burst firing were 0.22 ± 0.068 Hz and 5.44 ± 1.89 mV, respectively ($n = 10$). On the top of each depolarization, and depending on each cell, 1–7 action potentials were discharged (on average 3.83 ± 1.72; $n = 10$).

The firing behavior of this group of neurons was characterized in current clamp using depolarizing injections of different amplitudes. Injection of small depolarizing current pulses (+20 pA) elicited spike trains (Figure 3B1). These cells discharged spikes continuously during the entire duration of the current pulse with an increased interspike interval during the spike train. Moreover, these cells had relatively brief action potentials and a complex after-hyperpolarization with two clear components (Figure 3B2). These characteristics are specific to previously described low-threshold spike (LTS) cells (Kawaguchi and Kubota, 1993; Gibson et al., 1999; Goldberg et al., 2004; termed ''intrinsically-burst firing'' in the Petilla classification). Indeed, the LTS nature of this cell type was also confirmed by injection of hyperpolarizing current: rebound bursts of action potentials were observed after the current step (Figure 3B3). Such bursts at the offset of negative current injection, in the absence of a large sag voltage, are characteristic of a low-threshold T-type calcium conductance (Cauli et al., 1997; Goldberg et al., 2004), reported to be involved in generating pacemaker-like activity (Huguenard, 1996).

These neurons were also filled with biocytin and reconstructed (Figure 2D), revealing interneurons with a fusiform-shaped soma and an axonal plexus much larger than the dendritic tree. Axonal projections were dense in layer 4 and ascended to reach layer 1, where they often branched horizontally. Dendrites of these neurons were mostly restricted to layer 5, where some axonal projections were also present. The morphology of ascending axon interneurons was very similar, to those described before as ascending axon neurons (Lorente de Nó, 1922), Martinotti cells (Wang et al., 2004) or LTS cells (Kozloski et al., 2001; Goldberg et al., 2004).

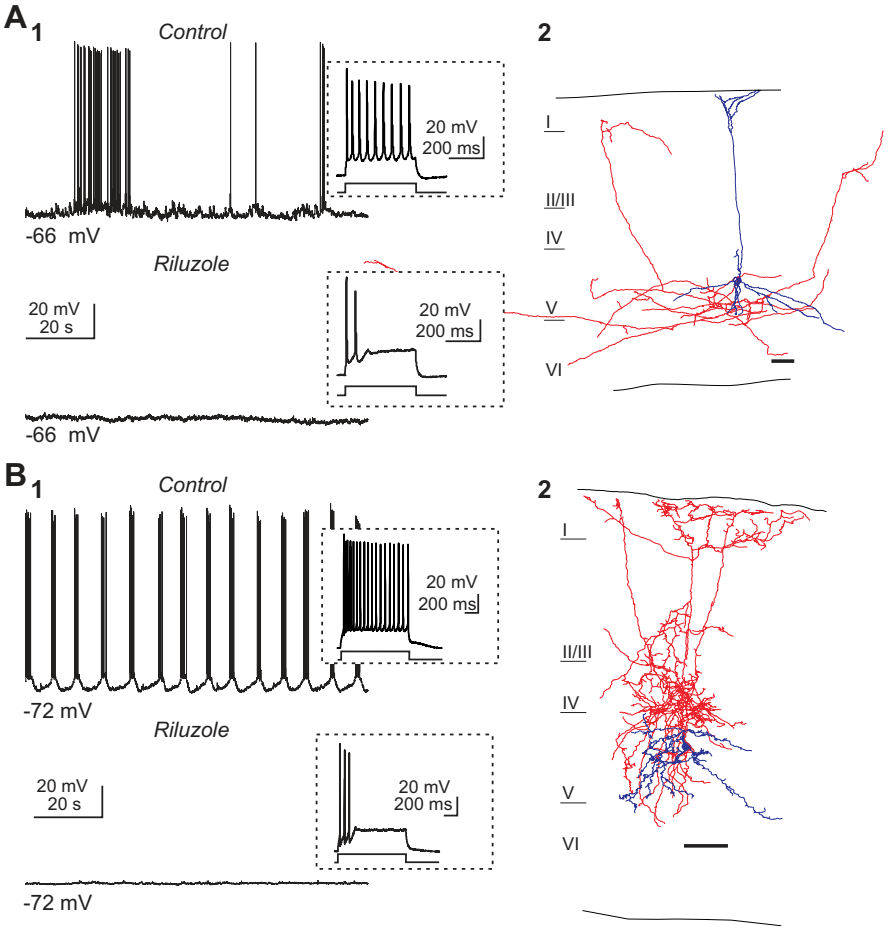

Figure 4. Persistent sodium current is essential for the persistent activity. *(**A**) Perfusion of riluzole (5 μM) abolished the spiking activity (**A1**) of a pyramidal neuron (anatomical reconstruction presented in **A2**). Inset displays the response induced by a small depolarizing current step. Note that a small current pulse was enough to elicit action potentials, suggesting that the fast Na^+ currents were not blocked. (**B**) Similar example of the effects of riluzole on the second subtype of intrinsically active neuron, a Martinotti cell (B2). Note how the slow oscillation (**B1**) in this interneuron (**B2**) is also completely blocked by riluzole.*

A persistent sodium current is necessary for the spontaneous activity

We then investigated the cellular mechanisms responsible for the persistent activity. We focused our attention on testing the role of persistent sodium currents, given the key involvement of this current in pacemaker behavior in the brain stem (Butera et al., 1999) and spinal chord (Darbon et al., 2004), and also, because of our past results demonstrating an effect of persistent sodium currents in the spontaneous network activity, as assayed with imaging (Mao et al., 2001).

For these experiments, we applied low concentration of riluzole (5–10 μM), an antagonist that selectively blocks the persistent sodium currents (Urbani and Belluzi, 2000), and used whole-cell recordings of type 1 and 2 neurons to test whether it affected the generation of persistent activity. Indeed, bath application of riluzole completely blocked spontaneous spiking activity in type 1 neurons and the spontaneous slow oscillation in type 2 neurons (**Figure 4**; $n = 10$). To ensure that riluzole didnot suppress the fast sodium current, short depolarizing current steps were also applied and the neurons responses were recorded. Importantly, under riluzole, neurons were still able to reliably fire action potentials (**Figure 4**, insets), indicating that the effect of this drug was not due to unspecific blockade of sodium channels. Moreover, we measured the amplitude of evoked action potentials and observed no change in spike amplitude for type 1 neuron (90.42 ± 6.52 mV in control condition and 90.62 ± 2.97 mV in presence of riluzole, $n = 3$) and a slight reduction in spike amplitude for the type 2 neuron (96.06 ± 2.08 mV in control condition and 91.33 ± 3.40 mV in riluzole, $p < 0.05$, $n = 6$) in presence of riluzole. These results, therefore, demonstrate that riluzole minimally affected the fast sodium current in our experiments. Note that riluzole affected the firing properties of both classes of cells in decreasing the number of action potentials evoked by a depolarized current pulse (preferentially in the late phase of the depolarizing step, see insets in **Figure 4**). Thus, like in other systems, persistent sodium currents appear crucial for the generation of spontaneous intrinsic activity in neocortex.

DISCUSSION

Using a novel imaging assay to detect neurons that are spontaneously active in the present of synaptic blockers, we have isolated two classes of neurons which display persistent, intrinsic activity in neocortex in the absence of excitatory or inhibitory synaptic inputs *in vitro*. One class comprises a subtype of interneuron that displays highly regular pacemaker-like activity while the other class shows irregular activity and is a subtype of pyramidal neuron. Moreover, we identify these neurons in primary sensory cortex, normally thought to be dominated by external sensory inputs.

Two subtypes of neocortical neurons are spontaneously active

To the best of our knowledge, our work represents the first survey for neurons that are spontaneously active in neocortical circuits in the absence

of synaptic transmission. Ours was an initial effort, restricted to primary visual cortex and describing those neurons that were most common, so it is quite likely that other classes of neurons, or neurons in other parts of the cortex, could have similar persistent activity properties. Our findings also may depend on the exact preparation and recording or experimental conditions, since we have only explored a limited number of variables. Nevertheless, it is quite notable that in this initial survey, out of the many dozens of subtypes of cortical neurons in mouse necortex (Lorente de Nó, 1922; see also www.columbia.edu/cu/biology/faculty/yuste for a catalog of reconstructions), all the spontaneously active cells detected belong solely to two specific subtypes of cells. Moreover, one of these two cell types had been previously implicated in regulating activity patterns in cortical circuits. This concordance cannot be coincidental and also, therefore endorses the validity of the approach as well as supporting the general idea that each subtype of cortical neuron may have a specific role in the circuit. More specifically, previous studies have demonstrated that ascending axon/Martinotti interneurons are reciprocally connected to layer 5 pyramidal cells, forming a feedback loop (Kozloski et al., 2001; Silberberg and Markram, 2007). Thus, the rebound excitation caused by the Martinotti inhibition onto several pyramidal neurons could trigger them to action potential threshold in a synchronized fashion. Moreover, because Martinotti cells receive strong, facilitating EPSPs from layer 5 pyramidal cells (Kozloski et al., 2001), this loop could endow the cortical microcircuit with a pacemaker kernel. Interestingly, neurons in layer 5 have also been implicated in the generation of epileptiform discharges (Connors, 1984) and cortical oscillations (Sanchez-Vives and McCormick, 2000). Moreover, neurons with low threshold firing properties are responsible for thalamic oscillations and thalamic epilepsy (Gutierrez et al., 2001; Llinás, 1987), so it is interesting that our intrinsically firing Martinotti neurons also have low-threshold firing. This disynaptic loop circuit thus appears ideally poised to generate persistent oscillatory activity and mediate oscillatory activity described *in vivo* (Steriade et al., 1993). Indeed, the frequency of the rhythmic oscillatory activity we observed in these interneurons closely corresponds to the slow oscillations described *in vivo* in the neocortex (Steriade et al., 1993).

Intrinsic mechanisms of persistent activity in neocortex

The specific patterns of discharge characterizing the persistently active neurons in neocortex are likely to be mediated by a multitude of ionic currents that shape the firing pattern. Nevertheless, we found one current crucial for the two types of pacemaker-like neurons, the persistent sodium current, although this does not necessarily mean that all the cortical neurons endowed with this particular current should behave similarly. Nevertheless, we would highlight that this is the same current that has been previously implicated in the generation of pacemaker activity in other parts of the brain. Specifically, persistent sodium currents are necessary for the generation of pacemaker-type activity in the breathing nucleus (Del Negro et al., 2002) and the spinal chord (Darbon et al., 2004), and the same antagonist, riluzole, at the same exact doses appears to have the same effect in the two types of neurons we have studied in neocortex. Thus, a current as ubiquitous as the persistent sodium current seems to have an important role for developing pacemaking properties in many brain areas.

In addition, our intracellular results confirm the initial observation we made on the effect of persistent sodium currents in blocking the generation of ensemble-type spontaneous activity in neocortex (Mao et al., 2001). In that work, the pharmacological blockade of persistent sodium channels dramatically reduced the number of spontaneously active neurons, as assay with calcium imaging of neuronal ensembles. Although in that early study we did not characterized morphologically or electrophysiologically the affected neurons, those population results are nicely complementary to those presented in **Figure 4** of our current study, which directly demonstrate the effect of blockers of persistent sodium currents on spontaneous action potentials.

Pacemaker-like neurons in cortical circuits

In considering the larger significance of our findings, we would emphasize that, in this novel survey, not only have we found pacemaker-like neurons in the neocortex but find at least two different types, located in several different layers. Our work is thus consistent with the proposal from Llinás that pacemaker neurons might be prevalent in central circuits (Llinás, 1987). We think it is appropriate to use the term pacemaker since not only is the phenomenological behavior of these neurons similar to that of other *bona-fide* pacemaker cells in the brain (activity in the absence of input and regular oscillatory activity whose frequency changes with membrane potential), but also, the current mechanisms responsible for this activity appear to be the same as those previously described in the midbrain and spinal chord. Given the limitations of the slice model, and the fact that we only imaged a small percentage of the neurons present in a slice, and that we used quite stringent criteria to detect active cells, it is likely that we are underestimating the number of pacemaker-like cells. Moreover, it should be highlighted that this initial survey was carried out in a primary sensory cortex, usually thought of as being input-driven. Thus, it is likely that the association or motor cortices could be endowed with a larger repertoire of pacemaker-like neurons.

The persistent spontaneous activity in the neocortex has not yet a clear demonstrated function. We could imagine that it may be used to pattern cortical responses to stimuli, or serve as excitatory kernels of intrinsic circuit dynamics. In any case, although the exact role of these pacemaker-like neurons and how these influence the normal and abnormal activity of the cortical microcircuitry remains to be elucidated, our results, revealing pacemaking-like activity in the midst of the cortical microcircuit, highlight the similarities between neocortical circuits and CPGs (Llinás, 1987 and 2001; Yuste et al., 2005).

CONFLICT OF INTEREST STATEMENT

The authors declare that the research was conducted in the absence of any commercial or financial relationships that should be construed as a potential conflict of interest.

ACKNOWLEDGMENTS

We thank R. Urban and J. Kelley for technical assistance and B. Watson, J. N. MacLean, T. Sippy, and A. Trevelyan for comments. This work was supported by the National Eye Institute. M. L. B.-J. was an OIF Marie Curie Fellow from the 6th European PCRD. We thank R. Llinás for his encouragement and support during the years. This study is dedicated to the memory of A. Alonso.

SUPPLEMENTARY DATA

A type 2 interneuron displaying pacemaker-like activity in V1. Representative calcium imaging movie of a slice bulk loaded with Oregon Green BAPTA 1 showing a cell ''blinking'' very regularly (on the top left). Subsequent targeted patching and characterization revealed it belonged to the class 2 type of neurons described in the study. Time resolution: 200 frame per second. Raw imaging data, displayed without any manipulation. This movie is attached to the on-line version of the paper found at the journal website, www.frontiersin.org/neuroscience.

REFERENCES

Aksay, E., Gamkrelidze, G., Seung, H. S., Baker, R., and Tank, D. W. (2001). In vivo intracellular recording and perturbation of persistent activity in a neural integrator. *Nat. Neurosci.* 4, 184–193.

Butera, R. J., Rinzel, J., and Smith, J. C. (1999). Models of respiratory rhythm generation in the pre-Botzinger complex. Bursting pacemaker neurons. *J. Neurophysiol.* 82, 382–397.

Brunel, N., and Wang, X. J. (2003). What determines the frequency of fast network oscillations with irregular neural discharges? I. Synaptic dynamics and excitation-inhibition balance. *J. Neurophysiol.* 90, 415–430.

Cauli, B., Audinat, E., Lambolez, B., Angulo, M. C., Ropert, N., Tsuzuki, K., Hestrin, S., and Rossier, J. (1997). Molecular and physiological diversity of cortical nonpyramidal cells. *J. Neurosci.* 17, 3894–3906.

Connors, B. W. (1984). Initiation of synchronized neuronal bursting in neocortex. *Nature* 310, 685–687.
Darbon, P., Yvon, C., Legrand, J. C., and Streit, J. (2004). INaP underlies intrinsic spiking and rhythm generation in networks of cultured rat spinal cord neurons. *Eur. J. Neurosci.* 20, 976–988.
Egorov, A. V., Hamam, B. N., Fransen, E., Hasselmo, M. E., and Alonso, A. A. (2002). Graded persistent activity in entorhinal cortex neurons. *Nature* 420, 173–178.
Gibson, J. R., Beierlein, M., and Connors, B. W. (1999). Two networks of electrically coupled inhibitory neurons in neocortex. *Nature* 402, 75–79.
Goldberg, J. H., Lacefield, C. O., and Yuste, R. (2004). Global dendritic calcium spikes in mouse layer 5 low threshold spiking interneurones: implications for control of pyramidal cell bursting. *J. Physiol.* 558, 465–478.
Goldman-Rakic, P. S. (1995). Cellular basis of working memory. *Neuron* 14, 477–485.
Grinvald, A., Arieli, A., Tsodyks, M., and Kenet, T. (2003). Neuronal assemblies: single cortical neurons are obedient members of a huge orchestra. *Biopolymers* 68, 422–436.
Gutierrez, C., Cox, C. L., Rinzel, J., and Sherman S. M. (2001). Dynamics of low-threshold spike activation in relay neurons of the cat lateral geniculate nucleus. *J. Neurosci.* 21, 1022–1032.
Huguenard, J. R. (1996). Low-threshold calcium currents in central nervous system neurons. *Annu. Rev. Physiol.* 58, 329–348.
Ikegaya, Y., Aaron, G., Cossart, R., Aronov, D., Lampl, I., Ferster, D., and Yuste, R. (2004). Synfire chains and cortical songs: temporal modules of cortical activity. *Science* 304, 559–564.
Ikegaya, Y., Le Bon-Jego, M., and Yuste, R. (2005). Large-scale imaging of cortical network activity with calcium indicators. *Neurosci. Res.* 52, 132–138.
Kawaguchi, Y., and Kubota, Y. (1993). Correlation of physiological subgroupings of non-pyramidal cells with parvalbumin- and calbindinD28k-immunoreactive neurons in layer V of rat frontal cortex. *J. Neurophysiol.* 70, 387–396.
Kenet, T., Bibitchkov, D., Tsodyks, M., Grinvald, A., and Arieli, A. (2003). Spontaneously emerging cortical representations of visual attributes. *Nature* 425, 954–956.
Kiehn, O., and Butt, S. J. (2003). Physiological, anatomical and genetic identification of CPG neurons in the developing mammalian spinal cord. *Prog. Neurobiol.* 70, 347–361.
Kozloski, J., Hamzei-Sichani, F., and Yuste, R. (2001). Stereotyped position of local synaptic targets in neocortex. *Science* 293, 868–872.
Llinás R. R. (1987) The intrinsic electrophysiological properties of mammalian neurons: insights into central nervous system function. *Science* 242, 1654–1664.
Llinás, R. R. (2001). I of the vortex: from neurons to self (MIT Press).
Lorente de Nó, R. (1922). La corteza cerebral del raton. *Trab. Lab. Invest. Bio.* 20, 41–78.
Lorente de Nó, R. (1938). Analysis of the activity of the chains of internuncial neurons. *J. Neurophysiol.* 1, 207–244.
Mao, B. Q., Hamzei-Sichani, F., Aronov, D., Froemke, R. C., and Yuste, R. (2001). Dynamics of spontaneous activity in neocortical slices. *Neurons* 32, 883–898.
Marder, E. (2000). Motor pattern generation. *Curr. Opin. Neurobiol.* 10, 691–698.
Peterlin, Z. A., Kozloski, J., Mao, B. Q., Tsiola, A., and Yuste, R. (2000). Optical probing of neuronal circuits with calcium indicators. *Proc. Natl. Acad. Sci.* 97, 3619–3624.
Sanchez-Vives, M. V., and McCormick, D. A. (2000). Cellular and network mechanisms of rhythmic recurrent activity in neocortex. *Nat. Neurosci.* 3, 1027–1034.
Shu, Y., Hasenstaub, A., and McCormick, D. A. (2003). Turning on and off recurrent balanced cortical activity. *Nature* 15, 288–293.
Silberberg G., and Markram H. (2007). Disynaptic inhibition between neocortical pyramidal cells mediated by Martinotti cells. *Neuron* 53, 735–746.
Smetters, D., Majewska, A., and Yuste, R. (1999). Detecting action potentials in neuronal populations with calcium imaging. *Methods* 18, 215–221.
Steriade, M., Nunez, A., and Amzica, F. (1993). A novel slow (<1 Hz) oscillation of neocortical neurons in vivo: depolarizing and hyperpolarizing components. *J. Neurosci.* 13, 3252–3265.
Urbani, A., and Belluzi, O. (2000). Riluzole inhibits the persistent sodium current in mammalian CNS neurons. *Eur J Neurosci.* 12, 3567–3574.
Tsiola, A., Hamzei-Sichani, F., Peterlin, Z., and Yuste, R. (2003). Quantitative morphologic classification of layer 5 neurons from mouse primary visual cortex. *J. Comp. Neurol.* 461, 415–428.
Wang, Y., Toledo-Rodriguez, M., Gupta, A., Wu, C., Silberberg, G., Luo, J., and Markram, H. (2004). Anatomical, physiological and molecular properties of Martinotti cells in the somatosensory cortex of the juvenile rat. *J. Physiol.* 561, 65–90.
Wang X. J. (2001). Synaptic reverberation underlying mnemonic persistent activity. *Trends Neurosci.* 24, 455–463.
Yuste, R., MacLean, J. N., Smith, J., and Lansner, A. (2005). The cortex as a central pattern generator. *Nat. Rev. Neurosci.* 6, 477–483.
Yuste, R., and Katz, L. C. (1991). Control of postsynaptic Ca2+ influx in developing neocortex by excitatory and inhibitory neurotransmitters. *Neuron* 6, 333–344.

doi:10.3389/neuro.01/1.1.009.2007